MNRAS **000**, 1–?? (2016) Preprint 28 July 2016 Compiled using MNRAS LATEX style file v3.0

The effects of host galaxy properties on merging compact binaries detectable by LIGO

R. O'Shaughnessy,[1]⋆ J. M. Bellovary,[2] C. R. Christensen,[3] S. Shen,[4] F. Governato,[5] A. Brooks[6]
[1]*Center for Computational Relativity and Gravitation, Rochester Institute of Technology, Rochester, NY 14623, USA*
[2]*Department of Physics, Queensborough Community College, Bayside, NY 11364, USA*
[3]*Department of Physics, Grinnell College, Grinnell, IA, 50112, USA*
[4]*Cambridge or Oslo?*
[5]*Department of Astronomy, University of Washington, Seattle, WA 98195, USA*
[6]*Rutgers, New Jersey*

Accepted XXX. Received YYY; in original form ZZZ

ABSTRACT
Cosmological simulations of galaxy formation can produce present-day galaxies with a large range assembly and star formation histories. A detailed study of the metallicity evolution and star formation history of such simulations can assist in predicting LIGO-detectable compact object binary mergers. Recent simulations of compact binary evolution suggest the compact object merger rate depends sensitively on the progenitor's metallicity. Rare low-metallicity star formation during galaxy assembly can produce more detected compact binaries than typical star formation. Using detailed simulations of galaxy and chemical evolution, we determine how sensitively the compact binary populations of galaxies with similar present-day appearance depend on the details of their assembly. We also demonstrate by concrete example the extent to which dwarf galaxies overabundantly produce compact binary mergers, particularly binary black holes, relative to more massive galaxies. We discuss the implications for transient multimessenger astronomy with compact binary sources.

Key words: keyword1 – keyword2 – keyword3

1 INTRODUCTION

Gravitational waves have been detected from coalescing black hole binaries (The LIGO Scientific Collaboration and the Virgo Collaboration 2016c,a). Over the next few years, ground-based gravitational wave detectors like LIGO and Virgo should detect the gravitational wave signal from many more similar merging compact binaries (The LIGO Scientific Collaboration and the Virgo Collaboration 2016a,b; Belczynski et al. 2016), as well as binary neutron stars and black hole-neutron star binaries (Abadie et al (The LIGO-Virgo Scientific Collaboration) 2010; Dominik et al. 2014). The host galaxies of gravitational wave sources will be identified, either directly or statistically. If the event is a merger of at least one neutron star, it is expected to be accompanied by detectable electromagnetic radiation via a number of mechanisms (see Fernández & Metzger 2016, and references therein) in addition to the strong gravitational wave signal. A multimessenger detection will pin down the sky position and therefore approximate birthplace of each merging binary (Nissanke et al. 2013). Even in the absence of well-identified electromagnetic counterparts, host galaxy information is still available from gravitational wave localization alone (Abbott et al. 2016; Singer et al. 2016). As GW detector networks increase in number and sensitivity, these localizations will allow statistical and, eventually, unique identification of host galaxies directly, even without associated electromagnetic emission. As with supernovae and GRBs, these host galaxy associations are expected to tightly constrain models for compact binary formation; see, for comparison, Maoz et al. (2011), Guetta & Piran (2007), Berger (2014), and references therein.

The host galaxies of distant short GRBs have already been extensively investigated, with the associations being used to draw preliminary conclusions about their progenitors (Berger 2014). Unlike GRBs, detected gravitational wave sources will be limited by the range of LIGO to the local universe; for example, binary neutron star sources should be closer than 400Mpc. Due to their proximity, each host galaxy can be explored at great depth and detail via position-resolved spectroscopy, enabling detailed position-resolved star-formation and chemical evolution histories (see,e.g. Kotulla et al. 2009; Canning et al. 2014; Pérez et al. 2013; González Delgado et al. 2015). However, unlike short GRBs and supernovae (SN), present-day compact binary populations can depend sensitively on rare low metallicity star formation. In this work, we assess by concrete example the extent to which detailed analysis of individual galaxies' assembly histories will be essential in investigations key physical questions about the origin of compact binary mergers.

This paper is organized as follows. In §2, we describe detailed hydrodynamical simulations of several galaxies, including four of

⋆ E-mail: oshaughn@mail.rit.edu

Milky Way-mass and two dwarfs. Though the four Milky Way-like galaxies are morphologically similar at $z = 0$, we show that their star formation and chemical evolution history have subtle but important differences due to their distinctive merger histories. To demonstrate these differences have a practical impact, in §3, we introduce a simple, metallicity-dependent phenomenological model to calculate the present-day rate and mass distribution of compact binary mergers from a galaxy's known history. In §4, we use this model to investigate the compact binary coalescence rate dependence on the galaxy's assembly history. In § 5 we discuss the implications of our study for the interpretation of host galaxy associations identified via transient multmiessenger astronomy, in the short and long term. We summarize our results in § 6.

2 COSMOLOGICAL SIMULATIONS

2.1 Simulating galaxy evolution

To thoroughly study the significance of low metallicity star formation, we examine cosmological smoothed particle hydrodynamics (SPH) N-body simulations of Milky Way-like galaxies with GASOLINE (Stadel 2001; Wadsley et al. 2004). These simulations allow us to analyze both spatially and temporally resolved star formation, and determine not only the metallicity history of compact object progenitors.

We selected our simulated regions of interest from a volume of uniform resolution, and resampled the region at very high resolution using the volume renormalization technique (Katz & White 1993). This technique allows us to follow the detailed physical processes involved in galaxy evolution in our selected region while still including large-scale torques from cosmic structure. Our cosmological parameters are $\Omega_0 = 0.24$, $\Omega_{\rm baryon} = 0.04$, $\Lambda = 0.76$, h = 0.73, $\sigma_8 = 0.77$ (Spergel et al. 2007) and model the ionizing UV background with the prescription from Haardt & Madau (1996). Our interstellar medium (ISM) model includes the non-equilibrium formation and destruction of H_2, which is incorporated in the cooling model along with metal lines (Christensen et al. 2012). Stars form probabilistically from gas particles which meet density ($n_{min} = 0.1$ amu cm^{-3}) and temperature ($T_{max} = 10^3$ K) thresholds. If a gas particle meets these criteria, it has a likelihood of forming a star particle (representing a simple stellar population with a Kroupa IMF (Kroupa 2001)) which is given by

$$p = \frac{m_{\rm gas}}{m_{\rm star}}(1 - e^{c^* {\rm X}_{\rm H_2} \Delta {\rm t}/{\rm t}_{\rm form}}) \quad (1)$$

where the star formation efficiency parameter c^* is set to 0.1 such that our galaxies match the observed Kennicutt-Schmidt law (Kennicutt 1989); X_{H_2} is the molecular hydrogen fraction of the gas particle; m_{star} and m_{gas} are the star and gas particle masses; [1] t_{form} is the dynamical time for the gas particle; and Δt is the time between star formation episodes, which we set to 1 Myr. A detailed study of different interstellar medium (ISM) models and the resulting star formation properties by Christensen et al. (2014b) demonstrates that this model allows star formation to occur in dense clumps of gas, in regions that correspond best to star formation in observed galaxies.

[1] Gas particles start with a set mass and may gain mass from feedback and lose it to star formation. Each star particle, when formed, has 1/3 of the progenitor mass of the forming gas particle. See Christensen et al. (2010) for a discussion of resolution issues in SPH simulations.

We model supernova feedback using the blastwave formalism described in McKee & Ostriker (1977) and implemented in our simulations as in Stinson et al. (2006). Each supernova releases $E_{SN} = 10^{51}$ erg into the surrounding gas with a radius determined by the blastwave equations. These particles are not allowed to cool for the duration of the blastwave, mimicking the snowplow phase of a supernova explosion. Previous works have found that this set of parameters results in realistic galaxies which obey a number of observed relations such as the mass-metallicity relation (Brooks et al. 2007), the Tully-Fisher relation (Governato et al. 2009), and the size-luminosity relation (Brooks et al. 2011), as well as reproduce the detailed characteristics of bulgeless dwarf galaxies (Governato et al. 2010) and the Milky Way (Guedes et al. 2011).

Also included in our simulations is a scheme for turbulent metal diffusion (Shen et al. 2010). Metals are created in supernova explosions and deposited directly to the gas within the blast radius. Stellar masses are converted to ages as described by Raiteri et al. (1996), and stars more massive than 8 $M_\odot$ are able to undergo a Type II supernova. We follow metal enrichment from both Type II and Type 1a supernova, with metal yields derived from Weaver & Woosley (1993) and Thielemann et al. (1986) respectively. From this point onwards metals diffuse through the surrounding gas, according to

$$\frac{dZ}{dt}|_{diff} = \nabla(D\nabla Z) \quad (2)$$

where the diffusion parameter D is given by

$$D = C_{diff}|S_{ij}|h \quad (3)$$

and h is the SPH smoothing length, S_{ij} is the trace-free shear tensor, and C_{diff} is a dimensionless constant which we set to a conservative value of 0.03.

We identify individual galaxies using the halo finder AHF (Gill et al. 2004; Knollmann & Knebe 2009), which identifies halos based on an overdensity criterion for a flat universe (Gross 1997). In each simulation, we are focusing on the stars which make up the primary (i.e. most massive) galaxy at $z = 0$.

2.2 Milky-Way-like galaxies with distinct histories

The evolution of a galaxy, in terms of its stellar mass and metallicity evolution, depends strongly on its interaction history. Galaxies which appear similar at the present day may have had drastically different histories, which may result in differences in compact object merger rates. To investigate whether galaxy history affects the compact binary event rate, we have chosen four simulations which are morphologically similar at $z = 0$ but differ strongly in their merger histories; see Figure 1.

The simulation h277 is a Milky Way analog with a quiescent merger history. It experiences its last major merger at $z = 3$, after which a small number of minor interactions permeate its life. This simulation has been shown to emulate several Milky Way properties, including stellar dynamics (Loebman et al. 2012, 2014; Kassin et al. 2014), baryon fraction (Munshi et al. 2013), halo properties (Zolotov et al. 2009, 2010), and disk structure (Brooks et al. 2011). It has a virial mass of $M_{vir} = 6.79 \times 10^{11} M_\odot$, stellar mass $M_* = 4.24 \times 10^{10} M_\odot$, and maximum circular velocity $v_{\rm circ} = 235$ km s^{-1}.

The simulation h258, on the other hand, has a much more active merger history. At $z = 1$ there is a 1:1 merger event; a gas disk rapidly reforms following the collision (see Governato et al. (2009)), resulting in a massive disk galaxy at $z = 0$ which looks remarkably similar to the Milky Way and to the other simulation,

h277. Prior to the $z = 1$ merger, each of the four progenitor galaxies actually experiences its own additional major merger events around $z = 3$. The combination of the series of major mergers, plus a number of minor interactions and flybys, gives a stark contrast to the relatively quiescent history of h277. At $z = 0$, h258 has a virial mass of $M_{vir} = 7.74\times10^{11}\,M_\odot$, stellar mass $M_* = 4.46\times10^{10}M_\odot$, and maximum circular velocity $v_{\rm circ} = 242$ km s^{-1}.

We include two additional Milky Way simulations with similar $z = 0$ properties, which have evolutionary histories that fall in between the extremes of the two described above. The galaxy h239 has a total virial mass of $M_{vir} = 9.3\times10^{11}\,M_\odot$, stellar mass $M_* = 4.50\times10^{10}M_\odot$, and maximum circular velocity $v_{\rm circ} = 250$ km s^{-1}. The galaxy h285 has a total virial mass of $M_{vir} = 8.82\times10^{11}\,M_\odot$, stellar mass $M_* = 4.56\times10^{10}M_\odot$, and maximum circular velocity $v_{\rm circ} = 248$ km s^{-1}. These galaxies are also described in Munshi et al. (2013); Bellovary et al. (2014).

Due to the differences in merger histories, the star formation histories and metallicity evolution of h258 and h277 also differ at early times. Figure 2 shows the star formation history (left panel) and metallicity evolution (right panel) of h277 (black) and h258 (red). The star formation histories are quite different at early times, where h277 has larger bursts of star formation between 2-4 Gyr, but h258 has a large burst at ~ 6 Gyr during a major merger. The right panel shows the mean metallicity of recently formed stars vs time (thick solid lines), where we define recent as within the past 50 Myr. The shaded regions correspond to one standard deviation of the mean, while the thick dashed lines represent the top and bottom 90%. We see that the early evolution of the metal properties of these galaxies does differ - between 0.5 and 6 Gyr, h277 hosts a *modestly* more metal-rich population than h258. For most astrophysical processes, the small metallicity difference illustrated here will have no impact on present-day observables. However, the population of binary black holes depends sensitively on all low metallicity star formation over cosmic time; as we show below, these small differences can have an observable impact at present.

2.3 Dwarf galaxies

We have also employed the results of detailed simulations for two dwarf galaxies: h603 and h516. The simulation of h603 consists of a low-mass disk galaxy (qualitatively similar to M33). It has a virial mass of $3.4\times10^{11}\,M_\odot$, stellar mass of $7.8\times10^{9}M_\odot$, and maximum circular velocity of 111 km s^{-1}. The structure and star formation of this galaxy has been extensively studied by Christensen et al. (2014a). We also include a bulgeless dwarf galaxy, h516, which has a disk with irregularly distributions star formation, with a virial mass of $3.8\times10^{10}M_\odot$, stellar mass $2.5\times10^{8}M_\odot$, and maximum circular velocity of 65 km s^{-1}. Images of these galaxies are shown in Figure 3, and we show their star formation history and metallitity evolution in Figure 4. Note that these galaxies have quite different masses, and are not meant to be directly comparable. The more massive h603 has a much more active star formation history and an overall increasing metallicity with time, whereas the less massive h516 is characterized by small bursts of star formation and a fairly flat metallicity evolution.

3 DETECTION-WEIGHTED COMPACT BINARY FORMATION

Our goal in this work is to estimate the *ratio* of compact binaries that should be merging, at present, in the two simulated Milky-Way analog galaxies described above as well as the dwarfs.

To explore plausible binary detection scenarios, we adopt a parameterized formalism for binary evolution and event detection in an individual galaxy, motivated by the detailed studies of PSG (O'Shaughnessy et al. (2008b)) and PSE (O'Shaughnessy et al. (2010)); similar approaches have been used by Lamberts et al. (2016) and others.

Binary evolution calculations suggest the binary compact object formation rate depends sensitively on the assumed metallicity, in conjunction with other parameters (see, e.g. Belczynski et al. 2010a; O'Shaughnessy et al. 2008a; Belczynski et al. 2016, and references therein). Gravitational wave detectors are also far more sensitive to massive compact binaries, which are preferentially formed in low metallicity environments (O'Shaughnessy et al. 2010; Dominik et al. 2014). As a result, low metallicity environments can be overwhelmingly efficient factories for detectable black hole binaries (Dominik et al. 2014; Belczynski et al. 2016). For this reason, our estimates for compact binary coalescence rates must account for how often different star-forming conditions occur; how often compact binaries that can coalesce now can derive from each environment; and how often LIGO will detect compact binaries with different masses, all other things being equal.

To characterize how much more likely LIGO will detect coalescing binaries with different masses, we use a common and naive estimate for the volume to which advanced LIGO is sensitive (see,e.g., O'Shaughnessy et al. 2010):[2]

$$V = \frac{4\pi}{3}[445{\rm Mpc}]^3 \int p(m_1,m_2|Z)dm_1dm_2[(\mathcal{M}_c/1.2M_\odot)^{5/6}]^3 \quad (4)$$

where $\mathcal{M}_c \equiv (m_1m_2)^{3/5}/(m_1+m_2)^{1/5}$. This expression depends explicitly on an assumed and metallicity-dependent mass distribution for compact object mergers, through the characteristic chirp mass $\mathcal{M}_{c*}(Z) \equiv [\int p(m_1,m_2|Z)dm_1d,m_2(\mathcal{M}_c/1.2M_\odot)^{15/6}]^{5/16}$. We calibrate our metallicity-dependent mass distributions to metallicity-dependent binary evolution calculations presented in Dominik et al. (2012) and Dominik et al. (2014). For neutron stars, we adopt a fiducial neutron star mass of $1.4M_\odot$ at all metallicities. For BH-NS binaries, we adopt a highly simplified model: the black hole masses are uniformly drawn from $5M_\odot$ to the maximum black hole mass $M_{max}(Z)$ allowed by *isolated* stellar evolution, as reported in prior work (see,e.g. Belczynski et al. 2016, and references therein). In agreement with much more detailed prior work Dominik et al. (2014), this simplified model yields typical chirp masses for BH-NS binaries that vary slightly as $Z/Z_\odot$ decreases, from a lower limit of $3M_\odot$ near solar metallicity to an upper limit of $4.3M_\odot$ in low-metallicity environments. Not least because the average chirp mass for BH-NS simply cannot vary dramatically, given the functional form of $\mathcal{M}_c$, our results for the BH-NS coalescence rate per unit galaxy mass do not depend sensitively on the choice of black hole mass distribution. Finally, for binary black holes, we

[2] For simplicity, in this calculation we neglect the effects of cosmology; strong field coalescence; and black hole spin; see Dominik et al. (2014), The LIGO Scientific Collaboration and the Virgo Collaboration (2016d), or The LIGO Scientific Collaboration and the Virgo Collaboration (2016b) for more details.

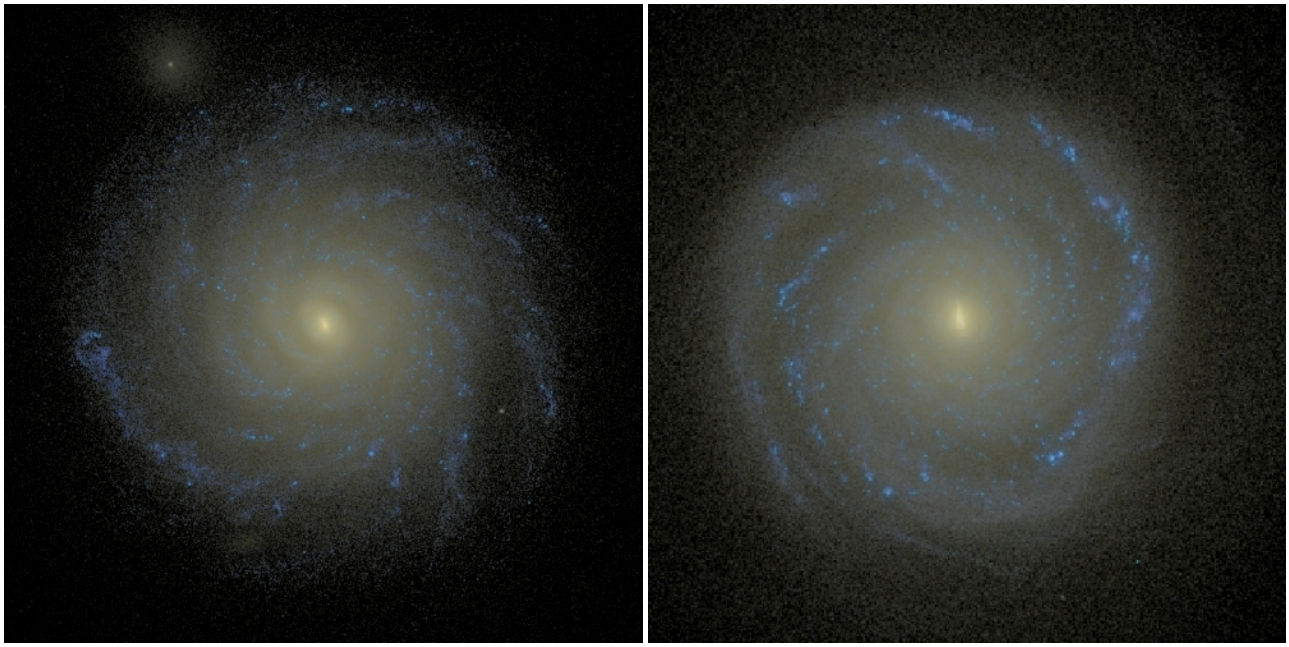

Figure 1. Synthetic SDSS gri images of two of our Milky Way-type galaxies, h277 (left) and h258 (right), created with SUNRISE (Jonsson 2006).

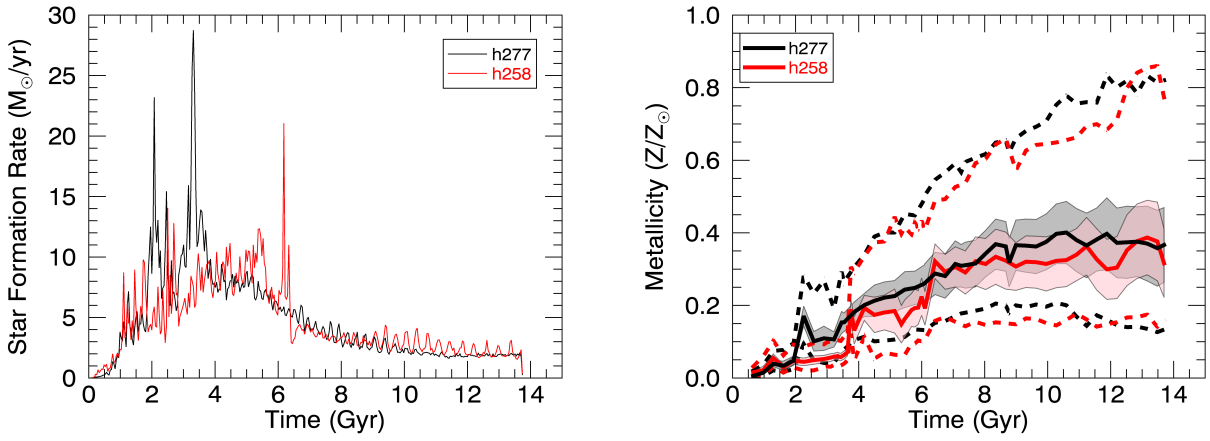

Figure 2. Star formation and metallicity versus time: *Left panel*: Star formation history $\dot{M}_*$ versus time. Black corresponds to h277 and red to h258. *Right panel*: A plot of the metallicity Z of recently-formed stars versus time. Solid red and black lines show the mean metallicity; dotted lines correspond to 90% of newly-born stars have lower metallicity, or 10% of newly-born stars have greater metallicity. When these two galaxies are 2 – 3Gyr old, prior to the first major merger of near the peak of their star-forming history, newly-born stars are created with significantly different metallicity. Additionally, prior to the second major merger of galaxy B at $\simeq$ 6Gyr, stars form in the h258 galaxy at a systematically lower metallicity than in the h277 counterpart.

assume comparable-mass binaries form ($m_1 = m_2$), with the distribution of component masses chosen to be $\propto m_1^{-p}$ between $5M_\odot$ and $M_{max}(Z)$ and zero otherwise, adopting a fiducial exponent $p = 2$; see, e.g., Dominik et al. (2013). For binary black holes, this means the detection-weighted mass distribution $[\propto p(m_1, m_2)\mathcal{M}_c{}^{15/6}]$ depends weakly on mass $[p(m_1, m_2)\mathcal{M}_c{}^{15/6} \propto m_1^{-0.5}\delta(m_1 - m_2)$. In our simple model, the total and chirp mass distributions are qualitatively consistent with detailed binary evolution calculations (Dominik et al. 2013).

To characterize the frequency of different star-forming conditions, we use our cosmological simulations of Milky Way-like galaxies, which provide each galaxy's star formation rate $\dot{M}_*$ and metallicity distribution $p(\log Z|t)$ over time (see Eqn. 7).

To characterize how often compact binaries form and coalesce, we use the ansatz adopted in PSE and PSG: for a star-forming parcel of mass ΔM the number of binaries born at time 0 which are coalescing now is $\lambda \Delta M dP_t/dt$, where λ is an overall efficiency per unit mass and $P_t(< t|Z)$ is a metallicity-dependent delay time distribution.[3] In this paper we are investigating the relative contribution of different star-forming environments and galaxy evolutionary

[3] For simplicity, we assume the mass and delay time distributions are uncorrelated. Figure A9 in PSG shows this approximation, while not strictly

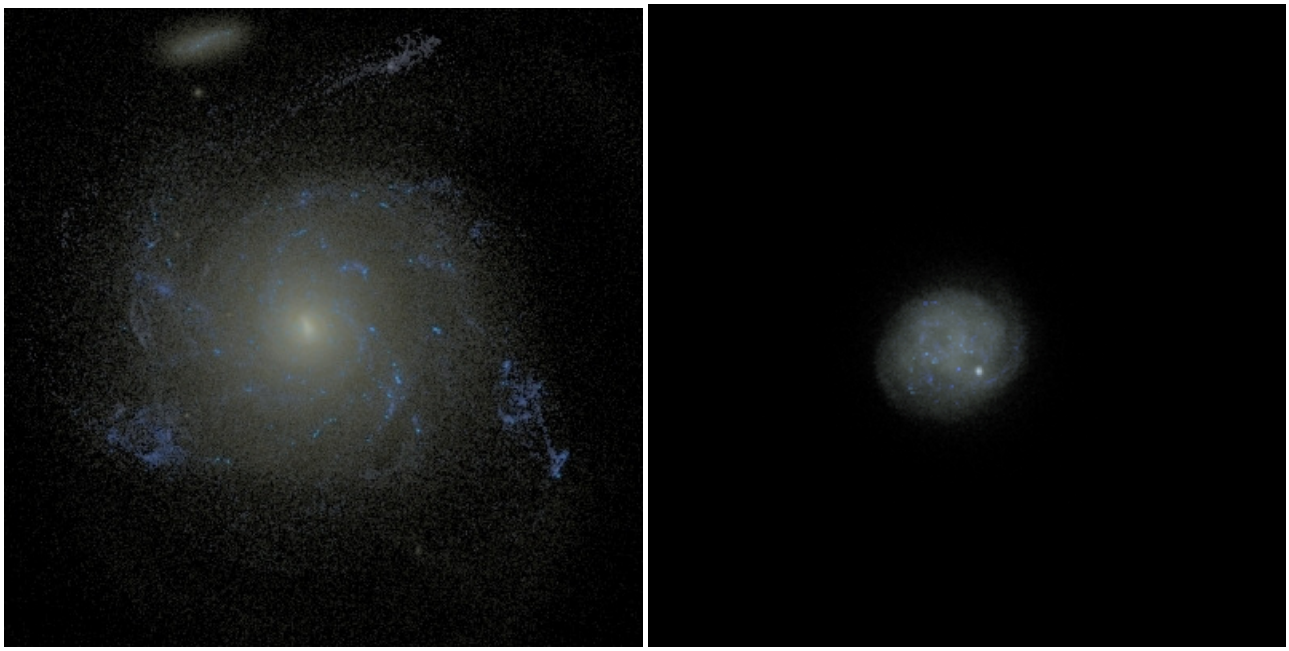

Figure 3. Synthetic SDSS gri images of our two lower-mass galaxies, h603 (left) and h516 (right - placeholder image, need image of h516), created with SUNRISE (Jonsson 2006).

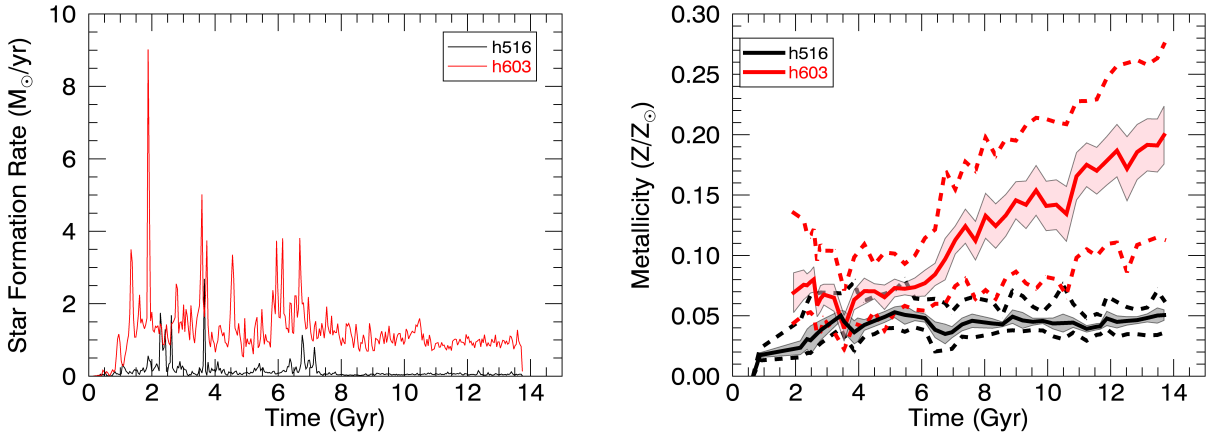

Figure 4. Star formation and metallicity versus time: *Left panel*: Star formation history $\dot{M}_*$ versus time. Black corresponds to h603 and red to h516. *Right panel*: A plot of the metallicity Z of recently-formed stars versus time. Solid red and black lines show the mean metallicity; dotted lines correspond to 90% of newly-born stars have lower metallicity, or 10% of newly-born stars have greater metallicity.

histories, not the overall normalization, so the overall scale of λ is irrelevant. However, to account for the strong tendency of low-metallicity star-forming regions to produce many binary compact objects, we adopt a power law

$$\lambda(Z) \quad = \quad \lambda_o \min[(Z/Z_\odot)^{-a}, F_{max}] \qquad (5)$$

with $a \in [0,3]$ and $F_{max} < 10^3$ (see, e.g.O'Shaughnessy et al. (2008a), BD2010). For the purposes of illustration, we adopt a concrete scale factor $\lambda_0 = 10^{-3}/M_\odot$, a typical value suitable for

true, is an excellent approximation for merging BH-BH binaries at solar metallicity.

neutron star compact binaries (see PSG, PSE, and BD2010). To calibrate the exponent, based on Tables 2 and 3 of Dominik et al. (2012) (model B), for binary black holes and black hole-neutron star binaries, we adopt $a = 1$, while for binary neutron stars we adopt $a = 0$; see, e.g., their Table 1 and Figures 5-7. This choice of exponent provides an extremely conservative assessment of the impact of low Z (see,e.g., O'Shaughnessy et al. 2012; Belczynski et al. 2016). For binaries containing neutron stars, for simplicity and without loss of generality we adopt the universal delay time distribution

$$\frac{dP_t(<t)}{dt} = \begin{cases} 0 & t < 10\text{Myr} \\ \frac{1}{t \ln(13\text{Gyr}/10\text{Myr})} & t \in [10\text{Myr}, 13\text{Gyr}] \end{cases} \qquad (6)$$

PSG and PSE show this distribution is reasonable approximations to compact binary delay time distributions.[4] For binary black holes forming at metallicities $Z < 0.25 Z_\odot$, we adopt the same prescription. For binary black holes formed near solar metallicity, the delay time distribution can favor long delays between birth and merger, as demonstrated in Figures 9 and 10 of PSE. [Figure 2 of Lamberts et al. (2016) is an extreme example of this well-known trend.] To be qualitatively consistent with detailed binary evolution calculations at near-solar metallicity (e.g., PSE and Belczynski et al. (2016)), for black holes forming at metallicities $Z > 0.25 Z_\odot$ we adopt a much more uniform delay time distribution, so coalescing black hole binaries have nearly uniform delay time distribution between 100Myr and 13Gyr; that said, our conclusions are not sensitive to this choice. For suitable choices of parameter, our phenomenological response function is qualitatively consistent with the results of detailed simulations of binary evolution (Belczynski et al. 2010b; Dominik et al. 2014, 2013, 2012).

Therefore, up to an irrelevant overall scale factor, the present-day detection-weighted coalescence rate r_D of binary compact objects formed by within two similar galaxies can be calculated via

$$r_D \propto \int d\log Z \int_{13\mathrm{Gyr}}^{0} dt V(Z)\lambda(Z)\frac{dP_t}{dt}(t)\dot{M}_* p(\log Z|t) \qquad (7)$$

4 COMPACT OBJECT BINARY FORMATION RATE

Our two Milky Way-like galaxies have extremely similar star formation histories and metallicity evolution, particularly at late times. However, at early times, the h258 galaxy forms stars for $\simeq$ 2Gyr at a lower characteristic metallicity ($Z \simeq 0.8\times10^{-3}$) compared to the h277 galaxy ($Z \simeq 2\times10^{-3}$). In this regime, the formation efficiency λ and sensitive volume V can depend sensitively on mass; for example, for binary black holes, the ratio of $(\lambda V)_{h277}/(\lambda V)_{h258} \simeq 3$.[5] However, in this same epoch, the star formation rate in the h258 (low-metallicity) galaxy is smaller, by a factor of roughly 2. Therefore, because only a fraction of order 10% of all star formation occurs in this epoch, by this order of magnitude argument, the overall number of present-day coalescing binary black holes in our two galaxies is expected to differ by of order ten percent. Using the concrete phenomenological calculations described above, we in fact find $(r_D/M)_{h277}/(r_D/M)_{h258} \simeq 0.9$.

The close agreement between the two galaxies' binary black hole populations, determined by the anticorrelation between star formation rate and metallicity, may be a single example of a broad trend. This anticorrelation could cause galaxies with similar present-day properties to always have similar present-day binary black hole populations, regardless of their detailed assembly histories. However, it is also possible that this close agreement is entirely a a numerical coincdence between the specific star formation rate and metallicities in these two galaxies. The effects described here are well within the scatter around the mass-metallicity relation. Marginally different realizations of these histories can easily produce factors of order unity difference in galaxies with otherwise indistinguishable present-day properties. That said, two other Milky-Way-like galaxies (h239 and h285) also show very similar binary black hole coalescence rates r_D/M; see Table 1.

Simulation	BHBH	BHNS	NSNS	$M_*(M_\odot)$
h277	0.0224	0.000247	0.000206	4.24×10^{10}
h258	0.0216	0.000297	0.000228	4.46×10^{10}
h239	0.023	0.000354	0.000268	4.50×10^{10}
h285	0.0236	0.000284	0.000241	4.56×10^{10}
h603	0.0381	0.000308	0.000441	7.8×10^{9}
h516	0.0949	0.000257	0.000884	2.5×10^{8}

Table 1. Event rates per unit mass r_D/M, arbitrary units, for the three different types of binaries discussed, along with the stellar mass of each galaxy.

More broadly, Table 1 shows the results of our calculations for the three types of compact binaries described above. These calculations show just how dramatically different the compact binary populations of galaxies with different present-day masses could be. In particular, dwarf galaxies have an exceptionally large fraction of low-metallicity star formation in their history (Kirby et al. 2013). The precise details of their chemical evolution can modify their present-day binary black hole binary populations by factors of order a few, despite adopting the conservative choices described above for the dependence of rate on metallicity.

To highlight how sensitively compact binaries depend on detailed evolutionary trajectories, Table 1 shows results for binary neutron stars. By our construction, no metallicity dependence is included in the present-day event rate for neutron stars. Thus, the differences in present-day state between these two galaxy population models arise solely and exclusively on the time distribution history of past star formation. In general, the present-day population depends often significantly (i.e., tens of percent) on the assembly history alone, even aside from any composition-dependent effects.

5 IMPLICATIONS FOR TRANSIENT MULTIMESSENGER ASTRONOMY

While a gravitational wave detection provides detailed information about merging objects (i.e. masses, spins, distance), we need further knowledge to understand the actual origins of the progenitors. Even when electromagnetic counterparts are available, the long delay times between binary formation and merger limit the prospects of examining the environment where the binary first formed. On the one hand, compact binaries are kicked by supernovae, moving substantially away from their birth position (Fong & Berger 2013; Berger 2014). On the other hand, particularly during the early epoch of galaxy formation, galaxies are well-mixed: stars and adjacent gas generally do not have similar chemical composition. These mixing effects have been previously recognized as an obstacle to interpreting transient event spectra. For example, Pontzen et al. (2010) previously demonstrated that absorbing gas neighboring transient events (there, long GRBs) would generally have high metallicity, even for low-metallicity progenitors. Pontzen et al. (2010) have previously used hydrodynamical simulations to demonstrate that observed ambient metallicities (there, using damped Lyman α absorbers in the host) do not tightly constrain the metallicity distribution of the progenitor; see, e.g., their Fig 3. Thus, the metallicity of stars and gas adjacent to a specific merger event provides few direct, unambiguous clues to a compact binary merger's progenitors.

[4] Simulations suggest the delay time distribution varies from model to model and with mass. These variations have less impact on our results than the evolving metallicity distribution of star forming gas.

[5] Adopting a more extreme exponent for the metallicity dependence ($a = 2$) only changes this ratio by of order 2.

Fortunately, with the advent of IFUs and position-resolved spectroscopy, observers can now probe the star formation history and metallicity of individual gas packets at different points in a galaxy. These highly-detailed probes will be essential tools to develop a comprehensive model of the galaxy's merger and chemical evolution history. Obtaining the galaxy-wide evolutionary history can help us infer compact binary formation conditions by identifying the lowest-metallicity formation events using stellar archaeological techniques. These techniques have been applied with great success to other transient events. For example, in several cases the metallicity of gas neighboring a long GRB (Modjaz et al. (2008); Levesque et al. (2010)) has been directly measured. The precise host offset can be compared to the distribution of light and star formation (Fong et al. 2010). Finally, on a host-by-host basis, the delay time between birth and merger has been constrained for short GRBs (Leibler & Berger 2010) and SN Ia (Maoz et al. 2011); see, e.g., the review in Berger (2014).

Thus, despite the challenges involved in obtaining sufficient statistics, possibly requiring third-generation instruments to obtain sufficiently many associations, past experience suggests host galaxy associations will provide unique clues into the formation mechanism of compact binaries. Each host galaxy associates a merger to a unique star formation history and metallicity distribution. With many events, these associations can potentially determine the "response function" for compact binaries: how often star forming gas of a given metallicity evolves into merging compact binaries.

6 CONCLUSIONS

We examine the present-day populations of coalescing compact binaries in galaxies with different assembly histories. We combine detailed and state-of-the-art cosmological simulations of galaxies with a simple but robust phenomenological model for how compact binaries form from different environments. We demonstrate that galaxies which appear similar at $z = 0$ but have differing merger histories will have somewhat different detection-weighted compact binary coalescence rates.

For binary black hole mergers in particular, we show that the present-day binary black hole coalescence rate for our two Milky-Way like galaxies is nearly identical, independent of their highly distinctive early-time formation histories. This result perhaps comes as somewhat of a surprise, considering the early differences in stellar and chemical evolution. Our calculations adopt the same framework as prior investigations, which demonstrated that black hole merger rates depend sensitively on low-metallicitiy environments (see,e.g. O'Shaughnessy et al. 2010; Dominik et al. 2013; Belczynski et al. 2016). More broadly, because compact binaries can merge long after they form, their host galaxy can evolve substantially in composition between birth and merger. Nonetheless, the apparent anticorrelation between the star formation rate and metallicity evolution of our galaxies has led to similar late-time populations, despite substantial differences early on. Further investigation is critical to assess whether this similarity is retained for more generic galaxy assembly histories and binary formation models. Now that we have introduced this method as a proof-of-concept here, it can be applied to large volume simulations, such as Illustris, EAGLE, or Romulus, in order to examine large numbers of galaxies and thus obtain statistically significant results.

The detailed analysis of the compact binary populations formed through the assembly history of individual galaxies is complementary to the population-based approach reported in Lamberts et al. (2016). More broadly, our analysis reflects similar theoretical studies performed in the interpretation of, for example, long GRBs and their host galaxies. For example, Kocevski et al. (2009) demonstrated that a sufficiently strong bias towards low-metallicity star formation would predict most events in the local universe occur low-mass and dwarf galaxies. For less extreme metallicity biases, subsequent calculations by Niino (2011) demonstrated that the metallicity distribution within galaxies will usually lead to events in a wide range of host galaxies in the local universe.

In short, in this work we have demonstrated that the confounding effects of host galaxy assembly history can in the near term complicate the interpretation of associations between GW sources and candidate host galaxies. However, given sufficient statistics, as will inevitably become available with next-generation GW instruments, combined with large-scale multiband followup, these confounding challenges can both be overcome and converged into opportunity. In the far future, with hundreds of thousands of thousands to millions of events per year in networks like Cosmic Voyager, Einstein Telescope, and DECIGO, GW measurements could even provide complementary statistical probes of the past history of galaxy assembly and evolution.

ACKNOWLEDGEMENTS

ROS acknowledges support from NSF award AST-1412449, via subcontract from the University of Wisconsin-Milwaukee, and PHY-1505629. JB acknowledges generous support from the Helen Gurley Brown Trust. A portion of this work was performed at the Aspen Center for Physics, which is supported by National Science Foundation grant PHY-1066293.

REFERENCES

Abadie et al (The LIGO-Virgo Scientific Collaboration) J., 2010, CQG, 27, 173001
Abbott B. P., et al., 2016, Living Reviews in Relativity, 19
Belczynski K., Holz D. E., Fryer C. L., Berger E., Hartmann D. H., O'Shea B., 2010a, ApJ, 708, 117
Belczynski K., Dominik M., Bulik T., O'Shaughnessy R., Fryer C., Holz D. E., 2010b, ApJ, 715, L138
Belczynski K., Holz D., Bulik T., O'Shaughnessy R., 2016, Nature, 534, 512
Bellovary J. M., Holley-Bockelmann K., Gültekin K., Christensen C. R., Governato F., Brooks A. M., Loebman S., Munshi F., 2014, MNRAS, 445, 2667
Berger E., 2014, ARA&A, 52, 43
Brooks A. M., Governato F., Booth C. M., Willman B., Gardner J. P., Wadsley J., Stinson G., Quinn T., 2007, ApJ, 655, L17
Brooks A. M., et al., 2011, ApJ, 728, 51
Canning R. E. A., et al., 2014, MNRAS, 444, 336
Christensen C. R., Quinn T., Stinson G., Bellovary J., Wadsley J., 2010, ApJ, 717, 121
Christensen C., Quinn T., Governato F., Stilp A., Shen S., Wadsley J., 2012, MNRAS, 425, 3058
Christensen C. R., Brooks A. M., Fisher D. B., Governato F., McCleary J., Quinn T. R., Shen S., Wadsley J., 2014a, MNRAS, 440, L51
Christensen C. R., Governato F., Quinn T., Brooks A. M., Shen S., McCleary J., Fisher D. B., Wadsley J., 2014b, MNRAS, 440, 2843
Dominik M., Belczynski K., Fryer C., Holz D., Berti B., Bulik T., Mandel I., O'Shaughnessy R., 2012, ApJ, 759, 52
Dominik M., Belczynski K., Fryer C., Holz D. E., Berti E., Bulik T., Mandel I., O'Shaughnessy R., 2013, ApJ, 779, 72
Dominik M., et al., 2014, Submitted to ApJ (arXiv:1405.7016)

Fernández R., Metzger B. D., 2016, Annual Review of Nuclear and Particle Science, 66, annurev
Fong W., Berger E., 2013, ApJ, 776, 18
Fong W., Berger E., Fox D. B., 2010, ApJ, 708, 9
Gill S. P. D., Knebe A., Gibson B. K., 2004, MNRAS, 351, 399
González Delgado R. M., et al., 2015, A&A, 581, A103
Governato F., et al., 2009, MNRAS, 398, 312
Governato F., et al., 2010, Nature, 463, 203
Gross M. A. K., 1997, PhD thesis, UNIVERSITY OF CALIFORNIA, SANTA CRUZ
Guedes J., Callegari S., Madau P., Mayer L., 2011, ApJ, 742, 76
Guetta D., Piran T., 2007, submitted to JCAP (astro-ph/0701194)
Haardt F., Madau P., 1996, ApJ, 461, 20
Jonsson P., 2006, MNRAS, 372, 2
Kassin S. A., Brooks A., Governato F., Weiner B. J., Gardner J. P., 2014, ApJ, 790, 89
Katz N., White S. D. M., 1993, ApJ, 412, 455
Kennicutt Jr. R. C., 1989, ApJ, 344, 685
Kirby E. N., Cohen J. G., Guhathakurta P., Cheng L., Bullock J. S., Gallazzi A., 2013, ApJ, 779, 102
Knollmann S. R., Knebe A., 2009, ApJS, 182, 608
Kocevski D., West A. A., Modjaz M., 2009, ApJ, 702, 377
Kotulla R., Fritze U., Weilbacher P., Anders P., 2009, MNRAS, 396, 462
Kroupa P., 2001, MNRAS, 322, 231
Lamberts A., Garrison-Kimmel S., Clausen D., Hopkins P., 2016, preprint, (arXiv:1605.08783)
Leibler C. N., Berger E., 2010, ApJ, 725, 1202
Levesque E. M., Kewley L. J., Berger E., Zahid H. J., 2010, AJ, 140, 1557
Loebman S. R., Ivezić Ž., Quinn T. R., Governato F., Brooks A. M., Christensen C. R., Jurić M., 2012, ApJ, 758, L23
Loebman S. R., et al., 2014, ApJ, 794, 151
Maoz D., Mannucci F., Li W., Filippenko A. V., Della Valle M., Panagia N., 2011, MNRAS, 412, 1508
McKee C. F., Ostriker J. P., 1977, ApJ, 218, 148
Modjaz M., et al., 2008, AJ, 135, 1136
Munshi F., et al., 2013, ApJ, 766, 56
Niino Y., 2011, MNRAS, 417, 567
Nissanke S., Kasliwal M., Georgieva A., 2013, ApJ, 767, 124
O'Shaughnessy R., Kopparapu R., Belczynski K., 2008a, arXiv:0812.0591
O'Shaughnessy R., Kalogera V., Belczynski C., 2008b, ApJ, 675, 566+
O'Shaughnessy R., Kalogera V., Belczynski K., 2010, ApJ, 716, 615
O'Shaughnessy R., Kopparapu R. K., Belczynski K., 2012, Classical and Quantum Gravity, 29, 145011
Pérez E., et al., 2013, ApJ, 764, L1
Pontzen A., et al., 2010, MNRAS, 402, 1523
Raiteri C. M., Villata M., Navarro J. F., 1996, A&A, 315, 105
Shen S., Wadsley J., Stinson G., 2010, MNRAS, 407, 1581
Singer L. P., et al., 2016, preprint, (arXiv:1603.07333)
Spergel D. N., et al., 2007, ApJS, 170, 377
Stadel J. G., 2001, PhD thesis, AA(UNIVERSITY OF WASHINGTON)
Stinson G., Seth A., Katz N., Wadsley J., Governato F., Quinn T., 2006, MNRAS, 373, 1074
The LIGO Scientific Collaboration and the Virgo Collaboration 2016a
The LIGO Scientific Collaboration and the Virgo Collaboration 2016b, Submitted to ApJ; available at http://arxiv.org/abs/1602.03842,
The LIGO Scientific Collaboration and the Virgo Collaboration 2016c, Phys. Rev. Lett., 16, 061102
The LIGO Scientific Collaboration and the Virgo Collaboration 2016d, ApJ, 818, L22
Thielemann F.-K., Nomoto K., Yokoi K., 1986, A&A, 158, 17
Wadsley J. W., Stadel J., Quinn T., 2004, New Astronomy, 9, 137
Weaver T. A., Woosley S. E., 1993, Phys. Rep., 227, 65
Zolotov A., Willman B., Brooks A. M., Governato F., Brook C. B., Hogg D. W., Quinn T., Stinson G., 2009, ApJ, 702, 1058
Zolotov A., Willman B., Brooks A. M., Governato F., Hogg D. W., Shen S., Wadsley J., 2010, ApJ, 721, 738